Theoretical Examination of Efficiency of Anthocyanidins as Sensitizers in Dye-Sensitized Solar Cells

Ibrahim Olasegun Abdulsalami*[a], Banjo Semire.[b], Isa Adewale Bello I. A[b].

[a] Department of Chemical Sciences, Fountain University, Osogbo, Nigeria.

[b] Department of Pure and Applied Chemistry, Ladoke Akintola University of Technology, Ogbomoso, Nigeria[2].

E-mail addresses: aiboldkip@gmail.com*; semireban@gmail.com; iabello90@yahoo.com.

*Corresponding author.

ABSTRACT

The function of the dye-sensitized solar cells dye-sensitized solar cells (DSSCs) has been traced down to the molecular level and the performance of the cell depends mainly on the positions and structures of the energy levels in the dye, semiconductor and electrolyte. Several metal free organic compounds have been designed, synthesized and applied as sensitizers in DSSCs, including anthocyanidins. However, some drawbacks concerning these applications are low efficiency and stability of the DSSCs. Thorough understanding of the electronic factors that contribute to light absorption is necessary, to select chromophores whose structural characteristics maximize the overall performance of the DSSCs. This study investigated structural effects and electronic contributions of four anthocyanidins, cyanidin (Cy), delphinidin (Dp), malvidin (Mv) and pelargonidin (Pg), to improve the efficiency of DSSCs. Quantum chemical method, the density functional theory (DFT), have been used to calculate parameters such as frontier molecular orbitals, band gap energies, reactivity descriptors.

Molecular orbitals (MOs) surfaces showed that titanium dioxide (TiO_2) orbital was susceptible to nucleophilic attack. The HOMO of terminal hydroxyl groups in dye were susceptible to nucleophilic attacks at different degrees. MOs of dye-semiconductor showed intramolecular charge transfer from dye to TiO_2 upon photoexcitation of dye. Electronic properties of dyes showed maximum absorption transitions in this order Mv < Dp < Pg < Cy. Reactivity descriptors revealed relationship between light-harvesting-efficiency (LHE) and chemical hardness (η) for dye molecules in the order Cy < Pg < Dp < Mv.

Cy-sensitized solar cell has the highest efficiency among anthocyanidins and this is in agreement with reported empirical report.

Introduction

The idea behind the DSSC developed by Grätzel and co-workers (De Angelis, Fantacci, and Selloni, 2008), sometimes called the Grätzel solar cell, is to mimic one of the energy producing processes in nature; the process of photosynthesis in plants. In the DSSC technology the tasks of light absorption and charge carrier transport are separated, unlike in conventional silicon systems where the semiconductor assumes both tasks (Chang, Hsieh, Lu, Yeh, and Houng, 2011; Limimg and Guangyong, 2011). The light absorption is performed by a single layer of dye molecule (sensitizer) adsorbed onto the surface of a wide band gap oxide semiconductor (Frederik, 2006; Gupta, Mukhopadhyay and Narayan, 2010). Charge separation takes place at the interface via photo-induced electron injection from the dye into the conduction band of the solid semiconductor (Grätzel, 2004; Kima, Yelundura, Nakayashikia, Rounsavillea, and Meemongkolkiata, 2006; Manzhos *et al*., 2011). The DSSC is a low-cost solar cell, a photoelectrochemical system that is based on energy generation by a semiconductor, like titanium dioxide (TiO_2) formed between a photosensitized anode and an electrolyte (Chen *et al*., 2011). TiO_2 is advantageous to be used as semiconductor in the DSSC because it is abundant, low cost, biocompatible and non-toxic (Grätzel, 2004; Chen *et al*., 2011). The dye molecules capture the energy of sunlight (Zhang, Huang, Luo, and Meng, 2012), and the absorption leads to excitation of an electron from a low-energy state into a high-energy state of the dye (Seo *et al*., 2011). The excited electron can then rapidly be injected into the semiconductor. The charge transfer, i.e. transfer through the back-electrode, takes place in the semiconductor, and in this way the absorption is separated from the charge transport. This concept, process of light absorption being separated from the charge transport, differentiates this type of solar cells from the conventional silicon based solar cell. The DSSCs also have a number of other requirements to meet and these are stability of the combined system, the

separate components in their different states, have a long lifetime and have high efficiency (De Angelis, Umari, Pastore, and Stefano, 2013).

However, the potential of DSSCs is far from being fully exploited, and the desire to improve the performance requires a deeper understanding of the involved processes, and knowledge accrued from the elucidation of the frontier molecular orbitals of the dye molecules in terms of electronic transfer would be of great assistance. Thorough understanding of the electronic factors that contribute to light absorption is necessary to select chromophores whose structural characteristics maximize DSSCs' performance (Gregory *et al*., 2011). Thus, in this article theoretical studies, such as the electronic absorption and alignment, light harvesting efficiency (LHE) and global descriptors of the dye molecules, semiconductor and the dye-semiconductor couples were investigated using density functional theory (DFT)/B3LYP/6-31G (d,p) level. The B3LYP functional was used in all calculations performed, this functional has proven successful for molecular system as well as condensed phase studies (Lundqvist *et al.,* 2006) and appears to be a good choice for studies of molecular adsorbates at metal oxides.

The function of the DSSC has been traced down to the molecular level and the performance of the cell has been reported to depend mainly on the positions and structures of the energy levels in the dye molecule, semiconductor and electrolyte (De Angelis *et al*., 2013). The molecular and electronic structures of the interface are of huge importance for understanding and controlling the mechanism of the electron transfer across the interface (Jean-Luc *et al.*, 2017). The enlightenment of this basic mechanism is crucial for designing and building stable, efficient solar cells that can compete with the energy resources of today.

In DSSCs, the working electrode comprises of mesoporous network of TiO_2 nanocrystalline (5-15µm, thickness) covered with a dye monolayer; this working electrode is supported on conducting glass (transparent conducting oxide; TCO) (Maa *et al*., 2009). Different materials such as platinum, palladium and gold can be used as counter-electrode of the cell (Belessiotis and Delyannis, 2011). The gap between the electrodes is typically filled with a molten salt which contains a redox couple (A/A^-); this salt serves as a hole conductor (Wang *et al*., 2012), and iodide/tri-iodide (I^-/I_3^-) couple has been widely applied as an electrolyte because of its good stability and reversibility (Pooman and Mehra, 2007). In overall process, the DSSCs generate electrical energy from solar without suffering any permanent chemical transformation (Kelly and Meyer, 2001).

Upon the incidence of solar energy in form of photon, on the surface of the solar cell, an electron is photo-excited from highest occupied molecular orbital (HOMO) level to lowest unoccupied molecular orbital (LUMO) level in dye molecule which causes electron injection from excited dye into TiO_2 conduction band, the electron migrates through TiO_2 network toward the TCO substrate. The charge transfer and transport in molecular and organic materials is dominated by charge localization resulting from polarization of the medium and relaxation of molecular ions. As a result of weak intermolecular interactions, the carriers in these materials are strongly localized on a molecule, and transport occurs via a sequence of charge-transfer steps from one molecule to other, similar to the hopping between defects states in inorganic semiconductors or band gap states in amorphous inorganic semiconductors. The energies of localized states in organic conductors are widely distributed due to several causes: the fluctuation of the lattice polarization energies, dipole interactions, and molecular geometry fluctuations (Bisquert *et al.,* 2006).

Chemical reactions typically involve movement of electrons from an electron donor (a base, nucleophile or reducing agent) to an electron acceptor (an acid, electrophile or oxidizing agent). The shapes and energies of the orbitals that act as electron donors or electron acceptors provide considerable insight into chemical reactivity (Zhang *et al.,* 2012). The HOMO is most commonly assumed to be the electron-donor orbital and the LUMO is the relevant electron-acceptor orbital. These two are collectively referred to as the frontier molecular orbitals and most chemical reactions involve electron movement between these two. In the case of chemical selectivity, where more than one combination of reagents can react, the donor with the highest energy HOMO would give up its electrons most easily and be the most reactive. And opposite has been reported for the cases of electron-acceptor reagents (Yusuke *et al*., 2016), i.e. the reagents with the lowest energy LUMO energies were found to accept electrons most easily and be the most reactive. For a mixture of several donor and acceptor reagents, the fastest chemical reaction would be expected to involve the reagent combination that yields the smallest energy gap. Meanwhile, when a molecule has multiple reactive sites the energy of the orbital is useless as a guide to site selectivity, but the shape of the relevant orbital is important (Lungu *et al.*, 2010; Simon *et al*., 2014). The adsorption of different molecules and atoms on a metal oxide surface, such as TiO_2, can substantially affect the properties of surface and thereby modify the function of the system (De Angelis *et al.*, 2008; Okonkwo, 2010).

Anthocyanins are water-soluble glycosides of polyhydroxyl and polymethoxyl derivatives of 2-phenylbenzopyrylium or flavylium salts (Øyvind and Kenneth, 2006), and anthocyanins without sugar moiety are anthocyanidins the anthocyanidins that are commonly found in fruits are cyanidin (Cy), delphinidin (Dp), malvidin (Mv), pelargonidin (Pg), peonidin (Pn) and petunidin (Pt). These anthocyanidins differ by the hydroxylation and methoxylation pattern on their B-rings (Figure 1), and only few of them are found in their non-glycosylated form in plants (Andersen and Jordheim, 2006, Torgils, Rune and Øyvind, 2003; Simmonds, 2003; Sirukarumbur, Vijaya, Emmanuel, James, and Namadevan, 2011)). The main positions of the hydroxylation are 3, 5, and 7 in the A ring and 3' and 5' in the B ring (Figure 1) (Andersen and Jordheim, 2006, Øyvind and Kenneth, 2006). Even though there are around thirty (30) different anthocyanidins, approximately 90% of all anthocyanins are based on the six most common anthocyanidins; Cy, Dp, Mv, Pg, Pn) and Pt and their chemical structures are presented as Table 1. The substituent groups on the anthocyanin mainly influence reactivity and colour by changing the electron distribution on the molecule and in relation to stability, the anthocyanidins are less stable than the anthocyanins. The stability of the heterocyclic π-electron structure of these compounds depend on the substituted positions as well as on the substituents themselves (Allero and Afolayan, 2006). Different substituents have a marked effect upon the colour and reactivity of anthocyanins and these effects are rationalized on the basis of the electron-donating properties of the substituents (Xing-Yu *et al.,* 2015).
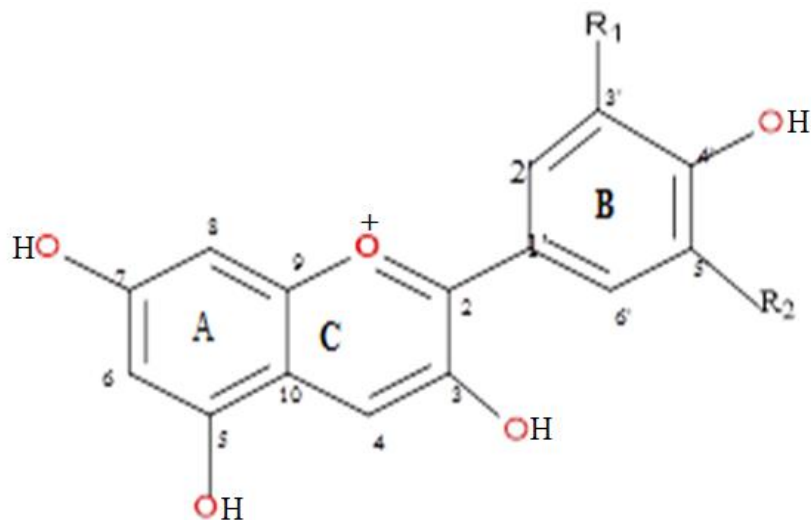
Figure 1: The basic structures of common anthocyanidins.

(Source: Øyvind and Kenneth, 2006)

Table 1: Chemical structure of the main anthocyanidins.

Name	Abbreviation	Substitution		Colour
		3'(R₁)	5'(R₂)	
Cyanidin	Cy	OH	H	orange/red
Delphinidin	Dp	OH	OH	blue/red
Malvidin	Mv	OMe	OMe	blue/red
Pelargonidin	Pg	H	H	orange
Peonidin	Pn	OMe	H	orange/red
Petunidin	Pt	OMe	OH	blue/red

3.0 Computational details

In this study the equilibrium geometries of the anthocyanidin dyes, semiconductor and dye-semiconductor couples were fully optimized at DFT level of theory with the standard 6-31G (d, p) basis set. The dye molecules (anthocyanidins), TiO_2 and the dye-semiconductor couples were modeled, optimized and their respective minimization energies were calculated, using

density functional theory (DFT)/B3LYP/6-31G (d,p) level. The B3LYP functional was used in all calculation performed by the author. This functional has proven successful for molecular system as well as condensed phase studies (Lundqvist *et al.,* 2006) and appears to be a good choice for studies of molecular adsorbates at metal oxides.

The accuracy of DFT calculations depend on the choice of the selected functional and basis sets, however polarized split-valence 6-31G(d,p) basis sets has proved to be sufficient and effective for calculating the excitation properties of organic dyes (Jacquemin *et al*., 2008). Introduction of additional diffuse functions in basis sets has negligible effects on the electron density. Frequency calculations are performed at the same levels of the theory to characterize the stationary points as local minima, none of the optimized dyes has imaginary frequency. The absorption transitions calculations are carried out on the optimized geometry in the ground S_0 state by TD-DFT/6-31G (d,p) theory in gas. The HOMO and LUMO levels are also calculated to give easy access to the calculation of molecular orbital and energies. All calculations were performed using Spartan 14 program implemented on an Intel® Core(TM) i5-5200U CPU @ 2.20GHz, 8G RAM computer. In order to analyze the electronic interaction between the adsorbates and the semiconductor in the complete system it is necessary to extract the energy levels with contributions from the adsorbate.

4.0   Results and discussion

4.1   Molecular geometry

The labelled optimized geometric structures of the dye molecules are presented as Figure 2. The structures are those of pelargonidin (Pg), cyanidin (Cy), delphinidin (Dp) and malvidin (Mv). These molecules have different substituents at C-14 and C15 (i. e. 3' and 5' of the B-ring c.f. Figure 1 and Table 1). Pg has –H atoms at these positions, Cy has H and –OH respectively, Dp has –OCH$_3$ and –OH respectively, and Mv has –OCH$_3$ at these positions. These structures also showed that on the C-ring, Pg has single -OH, Cy has two, Dp has three and Mv has two -OCH$_3$ and one -OH between them. The -OH group(s) on the C-ring of the Pg, Cy and Dp were in-plane and the -OCH$_3$ on the Mv are out-of-plane. The presence of -OH and -OCH$_3$ have significant roles to play in explaining the structural performance relationship of the anthocyanidins as sensitizers in the fabricated solar cells. The flavylium cation has electron

deficiency which makes the free anthocyanidins highly reactive (Hagberg *et al*., 2008). Pg and Mv have four number of phenolic hydroxyls, and the latter has –OCH$_3$ at two other places where Pg has –H atoms. Cy and Dp also five number of phenolic hydroxyls with different substitutions at C-14. These substitutions on the B-ring, particularly those located in the ortho- or the para-positions to the OH group, have been reported to influence the acidity of the hydroxyl group due to resonance and/or inductive effects (Øyvind and Kenneth, 2006). The implication is that since these dye molecules have similar (reactive) flavylium cation and different moieties at some positions, they are bound to have different chemical reactivities and selectivities.

4.2   Frontier molecular orbitals and band gap energies of the studied molecules.

It is imperative to examine highest occupied molecular orbital (HOMO) and lowest unoccupied molecular orbital (LUMO) energy levels of the molecules; dye molecules, semiconductor and dye-semiconductor couples. This is because the relative ordering of the occupied (HOMO) and virtual (LUMO) orbitals provides a reasonable qualitative indication of excitation properties for the organic dyes. The HOMO and LUMO energies of more efficient dye-sensitizers are essential to locate suitable values for tuning the conduction band edge of the semiconductor and redox potential of an electrolyte in DSSCs (De Angelis *et al*., 2013). The energy of the ground and the excited states of the dyes, together with the energies of the valence (VB) and conduction (CB) band edge for TiO$_2$ and the redox level of the I$_3^-$/I$^-$ electrolyte are presented as Figure 5. Figure 6 and Table 2 showed the HOMO, LUMO and band gap energies (E$_g$) of the dye-sensitizers in gas phase, and three other solvents. For all the calculations, energy of the excited state was obtained as of the sum of the energy of the ground state (HOMO) and the energy of the lowest singlet-to-singlet transition. Most chemical reactions involve electron movement between the HOMO and LUMO.

Figures 3 showed the contour plots of the frontier orbitals of the semiconductor and dye molecules, and Figure 4 showed those of dye-semiconductor couples. Table 2 contained the data obtained from the calculations of the electronic properties (HOMO, LUMO and band gap) of the anthocyanidins, semiconductor and the dye-semiconductor couples, in the gas phase, aqueous, ethanol and dimethyl sulphoxide. The band gap is associated with the probability of electronic excitation of a molecule. From these data the molecular orbital

surfaces of the dye molecules, semiconductor and the dye-semiconductor couples are explained in the following sub-sections.

4.2.1 Molecular orbital surfaces of semiconductor and dye molecules

From the Figure 3, the HOMO orbitals mainly overlay on the donor unit and the LUMO acceptor unit. The HOMO of the semiconductor (TiO_2) showed that the molecular orbital surface extend over titanium atoms. The oxygen atoms at the terminal have non-bonding characters. The other oxygen atoms contain weakly bonding characters, as their bonding orbitals contain surfaces that extend over the neighbouring titanium atoms. The molecular orbital for the LUMO orbitals of the atoms of TiO_2 were observed to be different from those of the HOMO as the LUMO orbitals contain nodes that divide the regions between oxygen and the titanium orbitals. The orbitals of terminal oxygen atoms were found to weakly bind with the neighbouring titanium atomic orbitals. The HOMO energy level of the molecules corresponds to the oxidation potential of a dye sensitizer (Semire, Oyebamiji & Odunola, 2017, Sean *et al*., 2016). This implies that the larger an oxidation potential, the higher will be the driving force for the reduction of oxidized dye (Jean-Luc *et al.,* 2017).

From the above information, TiO_2 molecular orbital is susceptible to electrophilic attack; addition of electrons to the non-bonding orbitals weakens the bonds and pushes (terminal oxygen) atoms apart, while removal of electrons from the orbitals of the TiO_2 molecule would have opposite effect. The terminal region of the molecule (i. e. oxygen) most electron rich, hence most susceptible to electrophilic attack, thus electron transfer (or movement) and bond formation is expected to occur at these terminal oxygen atoms. For the dye-sensitizers the HOMOs were extended over neighbouring atoms in the 'A' and part of 'C' rings in the cases of the Pg, Cy and Dp, but Mv. The HOMO orbitals of the terminal -OH were also observed to have characteristic nucleophilic attack susceptibility in the varying degrees; for Cy (in order of O2 > O6 > O5 > O4 > O3), Dp (in order of O2 > O6 > O7 > O5 > O4 > O3), Mv (in order of O2 > O6 > O5 > O4 > O3) and Pg (in order of O2 > O5 > O4 > O3), numbering of the atoms as shown in Figure 4.8. This implies that the orbitals of the terminal hydroxyl groups of these dye molecules are susceptible to nucleophilic attacks in the order explained above. However, the submission of Andrey and Neyde (2006) on the point of linkage between the semiconductor and dyes would require some scrutiny, as it is obvious from above that the points of linkage between the dye and the semiconductor are not restricted to positions 3' and

5' (R$_1$ and R$_2$) on the C-ring (Figure 2). Inferable from the molecular orbital surfaces of the dye molecules is that the hydroxyl groups can serve as point of attachments or linkage to the semiconductor. The degree of nucleophilic susceptibility vary from one end to another within the molecule. The results obtained showed that the oxygen atoms on the hydroxyl groups on the C-ring are most susceptible to nucleophilic attack than any other OH on any other rings. Observed trends in the LUMO orbitals of the dye molecules were in converse with respect to the trends in the HOMO orbitals; their HOMOs have molecular orbital surface extended over neighbouring atoms within the ring (π-extension) which are concentrated on the C-ring and the terminal hydroxyl orbitals showed non-bonding characteristics with orbitals of their respective neighbouring atoms. The LUMO has extension over the atomic orbitals of the atoms in the A- and B-rings.

4.2.2   Molecular orbital surfaces of the dye-semiconductor couples.

The contour plots of HOMO and LUMO orbitals of the dye-semiconductor couples are presented as Figure 4. These Figures showed two distinct molecular orbital surfaces of the dye-semiconductor couples. The molecular orbital surfaces, of the HOMO, were observed to extend over the atomic orbitals of neighbouring atoms of the dye molecules. For the LUMO, the molecular orbital surfaces were found to extend over the atomic orbitals of the semiconductor. Slight objection was also observed in the Mv-TiO$_2$ couple; the Ti and O atomic contain non-bonding characters. For the Pg-TiO$_2$ the HOMO orbitals showed that Pg served as the donor and that no atomic orbital of the TiO$_2$ displayed any form of non-bonding, bonding or anti-bonding character and the opposite was observed for in the LUMO orbitals of the couple. The HOMO orbitals of the Cy-TiO$_2$ couple extend over the neighbouring atomic orbitals of the titanium dioxide and the LUMO orbitals contain molecular orbital surfaces of the couple extended over 'B' and 'C' rings of the cyanidin molecule. For Dp-TiO$_2$ couple the HOMO orbitals contain molecular orbital surface extended over the terminal neighbouring atomic orbitals of the titanium. The LUMO orbital contain the molecular orbital surface extension over the neighbouring atomic orbitals of atoms in the 'B' and 'C' rings. The same was observed for the HOMO and LUMO orbitals and that the molecular orbital surface of the Mv-TiO$_2$ couple showed that the LUMO orbitals of the terminal titanium atomic orbitals contain non-bonding character. Jean-Luc et al., 2017 posited that for molecules that exhibit large energy differences between consecutive frontier electronic levels the electron transfer

(ET) process is generally dominated by the interaction between HOMOs and LUMOs of the donor and the acceptor, respectively. The electron distributions in the HOMO and LUMO of all studied derivatives clearly indicated that an intramolecular charge transfer from the donor moiety (anthocyanidin moiety) to the acceptor moiety (titanium dioxide) occurred upon photoexcitation of the dye.

The energy band gap values obtained for the dye molecules and TiO_2-dye couples (Table 2 and Figure 6) in the different media were such that in gas phase Mv < Cy = Pg < Dp, in aqueous phase Cy < Pg < Dp < Mv, in ethanol Dp < Cy < Pg <Mv and in DMSO Mv < Dp < Cy < Pg. For the dye-TiO_2 couples the energy band gap for the complexes showed Cy-TiO_2 < Dp-TiO_2 < Mv-TiO_2 < Pg-TiO_2. Most chemical reactions involve electron movement between the HOMO and LUMO, and closely related to chemical reactivity (reaction rate) is chemical selectivity (where more than one combination of substituents can react) it is expected that the donor with the highest HOMO would give up its electrons most easily and be the most reactive, and lowest LUMO energies would be expected to accept electrons most easily and be the most reactive. In this case it was observed by examining the energies of the frontier orbitals of the dye molecules in different media, where chemical reaction requires electron donation from the donor's HOMO, several donor and acceptor moieties, the fastest chemical reaction would be expected to involve the TiO_2-dye combination that yields the smallest energy gap. A related selectivity question arises when a molecule has multiple reactive sites. In this case, the energy of the orbital is useless as a guide to site selectivity, but the shape of the relevant orbital is important. This is also in good agreement with the empirical earlier reported by Abdulsalami et al., 2016.

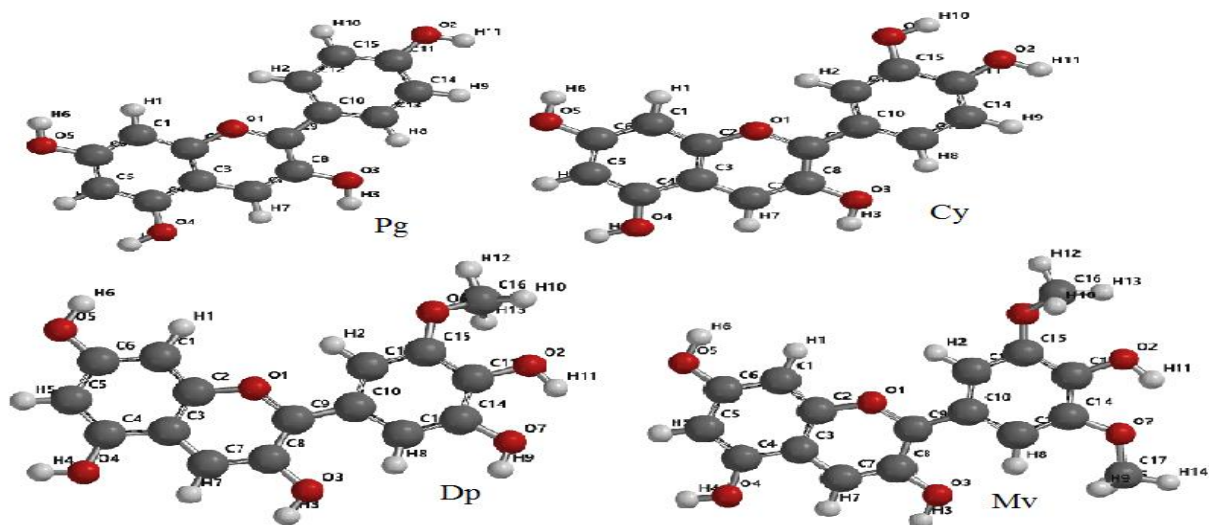Figure 2: Labelled optimized structures of the dye-sensitizers.

Note: Red ball = Oxygen atom; White ball = Hydrogen atom; Silver ball = Carbon atom.
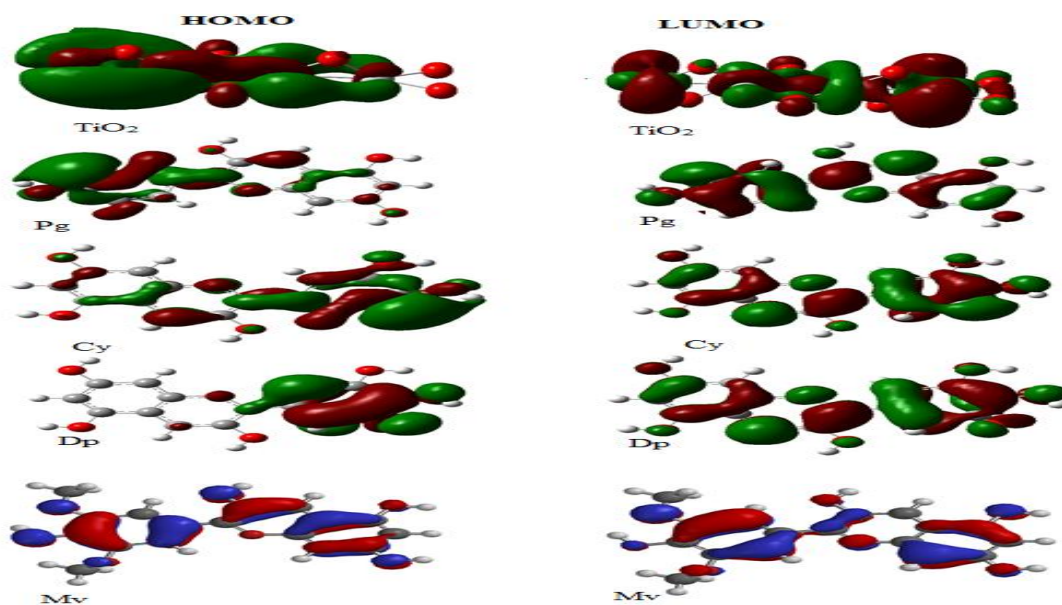

Figure 3: The contour plots of the HOMO and LUMO orbitals of the dye molecules and semiconductor.
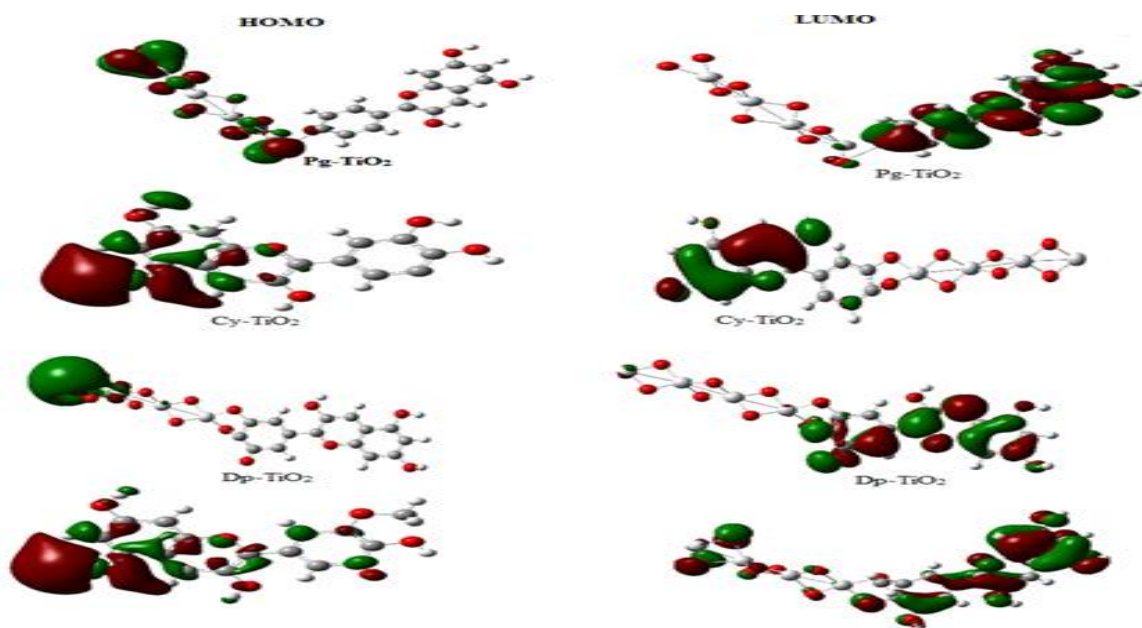
Figure 4: The contour plots of the HOMO and LUMO orbitals of the dye-semiconductor couples.

Table 2: Global reactivity descriptors for the studied molecules and light harvesting efficiency (LHE) for the dye-sensitizers in gas phase.

Sample	HOMO (eV)	LUMO (eV)	Eg (eV)	μ (eV)	η (eV)	ω (eV)	LHE
Pg(vac)	-9.40	-6.54	2.86	7.970	1.430	22.210	0.449
Cy(vac)	-9.13	-6.54	2.59	7.835	1.295	23.702	0.225
Dp(vac)	-8.98	-6.39	2.59	7.685	1.295	22.803	0.774
Mv(vac)	-8.88	-6.31	2.57	7.595	1.285	22.445	0.858
Pg(aq)	-5.75	-2.99	2.76	4.370	1.380	6.920	N/A
Cy(aq)	-5.68	-3.23	2.45	4.355	1.425	6.655	N/A

Dp$_{(aq)}$	-5.76	-2.97	2.79	4.365	1.395	6.829	N/A
Mv$_{(aq)}$	-5.78	-2.98	2.80	4.380	1.400	6.852	N/A
Pg$_{(EtOH)}$	-5.95	-3.01	2.94	4.480	1.470	6.827	N/A
Cy$_{(EtOH)}$	-5.83	-3.01	2.82	4.420	1.410	6.928	N/A
Dp$_{(EtOH)}$	-5.81	-3.04	2.77	4.425	1.385	7.069	N/A
Mv$_{(EtOH)}$	-5.97	-2.89	3.08	4.430	1.540	6.372	N/A
Pg$_{(DMSO)}$	-6.05	-3.12	2.93	4.585	1.465	7.175	N/A
Cy$_{(DMSO)}$	-5.94	-3.13	2.81	4.535	1.405	20.566	N/A
Dp$_{(DMSO)}$	-5.94	-3.18	2.76	4.560	1.380	20.794	N/A
Mv$_{(DMSO)}$	-5.89	-3.15	2.74	4.520	1.370	20.456	N/A
Pg-TiO$_2$	-6.875	-4.412	2.463	-	-	-	N/A
Cy- TiO$_2$	-7.794	-7.896	0.098	-	-	-	N/A
Dp- TiO$_2$	-4.473	-4.242	0.232	-	-	-	N/A
Mv- TiO$_2$	-4.394	-3.608	0.785	-	-	-	N/A

N/A = the data is not applicable to the parameter.

4.3   Electronic properties of the studied molecules.

Table 3 contains data obtained from the theoretical calculation of absorption peaks, oscillation strength and molecular orbitals that were involved in the electronic transitions of dye-sensitizers. The absorptions in visible and near-UV region of the spectrum are the most important regions for photo-current conversion, so only the singlet $\rightarrow$ singlet transitions of the absorption bands with the wavelength longer than 300 nm were recorded in explaining the electronic properties of the anthocyanidins studied in relation to their application as sensitizers. In Figure 5, the energy diagram comprising of the ground state (blue line) and the excited state

(red line), that is the HOMO and LUMO energies calculated for the dye-sensitizers and the dye-semiconductor couples. The conduction (red line) and valence (blue line) bands of the TiO_2, and the redox level of the I_3^-/I^- electrolyte (Reda *et al*., 2014) are also shown on the left and right hand sides, respectively. The dotted lines are drawn as aids to the eye for an easier examination of the energy level alignment. For all dyes, the LUMO lies above the conduction band edge of TiO_2, making possible the transfer of the photoelectron from the dye to the semiconducting oxide, the transfer is direct bandgap. In addition, the HOMO of all dyes lies below the redox level of the electrolyte, allowing for the transfer of the electron to the dye and its regeneration. The driving force of the electron injection from the dye into the semiconductor is the energy difference between the excited state of the dye and the conduction band edge of the oxide (Baetens *et al*., 2010). The microscopic information relating to the electronic transitions were obtained by examining the molecular orbital conforming to each electronic transition, as calculated using the TD-DFT/6-31G (d,p) level of theory as shown in Table 3. The absorptions in visible and near-UV region of the spectrum are the most important regions for photo-current conversion, so only the singlet $\rightarrow$ singlet transitions of the absorption bands with the wavelength longer than 300 nm are listed and discussed. The maximum absorption wavelengths (λ_{max}) for the dyes which correspond to HOMO$\rightarrow$LUMO (i.e. $\pi \rightarrow \pi^*$) transitions for Pg, Cy, Dp and Mv are 435.80 nm, 432.91 nm, 442.83 and 445.20 nm respectively. The λ_{max} for Pg arises from H – L (0.37), H – L (0.58) and H-1 – L (0.37). The λ_{max} for Cy arises from H-1 – L (0.69), H – L (0.61) and H-1 – L (0.22). For Dp the λ_{max} arises from H – L (0.61) and H-2 – L (0.23) and for Mv the λ_{max} arises from H – L (0.74) and H-2 – L (0.15). The λ_{max} for Pg, Dp and Mv arose from H – L, with more than about 60 % contributions from Pg and more 60 % contributions from Dp and Mv. However, that of Cy arose from H-1 – L and the H – L transition contributed slightly above 61 %. The absorption peaks of the dyes are assigned to $\pi - \pi^*$ type transitions. This means that electron transfer are predominantly from HOMO – LUMO transitions, corresponding to intra-molecular electron transfer direction substantially from the electron rich units to the electron withdrawing units. The maximum absorption transitions of the studied dye were found to be in decreasing order Mv < Dp < Pg < Cy.

Table 3: Calculated absorption peaks, oscillation strength and molecular orbitals (mos) involved in the electronic transitions of dye-sensitizers at TD-DFT B3LYP/6-31G (d.p)

| λ_{max} (nm)	f	MOs involved in transition
		Pg
256.36	0.2983	HOMO-4 → LUMO 41% , HOMO-1 → LUMO+1 38%
261.77	0.1057	HOMO → LUMO+1 54% , HOMO → LUMO+2 12%, HOMO-3 → LUMO 10%
314.56	0.0196	HOMO-3 → LUMO 10% , HOMO-3 → LUMO 73%
352.24	0.0382	HOMO → LUMO+1 19%
381.56	0.7393	HOMO-2 → LUMO 95%, HOMO-1 → LUMO 55%
435.80	0.4490	HOMO → LUMO 37% , HOMO → LUMO 58%, HOMO-1 → LUMO 37%
		Cy
262.73	0.0959	HOMO-4 → LUMO 47%, HOMO-1 → LUMO+1 23%, HOMO -> LUMO+2 17%
281.58	0.0611	HOMO → LUMO+1 64% , HOMO-1 → LUMO+1 21%
317.10	0.0158	HOMO-3 → LUMO 72%, HOMO → LUMO+1 19%
375.48	0.7215	HOMO-2 → LUMO 69%, HOMO → LUMO 23%
432.91	0.2205	HOMO-1 → LUMO 15 %, HOMO → LUMO 61%, HOMO-1 → LUMO 22%,
468.15	0.2684	HOMO-2 → LUMO 14%
		Dp
283.04	0.0737	HOMO → LUMO+1 38%, HOMO-4 → LUMO 24%, HOMO-1 -> LUMO+1 22%
300.14	0.0145	HOMO-4 → LUMO 66%, HOMO → LUMO+1 30%
337.30	0.1696	HOMO-3 → LUMO 79%
409.69	0.2878	HOMO-2 → LUMO 66%, HOMO → LUMO 25%
442.83	0.7446	HOMO → LUMO 61%, HOMO-2 → LUMO 23%
502.86	0.0182	HOMO-1 → LUMO 91%
		Mv
283.36	0.1158	HOMO → LUMO+1 45%, HOMO-4 → LUMO 27%
302.34	0.0131	HOMO-4 → LUMO 65%, HOMO → LUMO+1 32%
339.19	0.2102	HOMO-3 → LUMO 80%
412.48	0.1650	HOMO-2 → LUMO 73%, HOMO → LUMO 17%
445.20	0.8576	HOMO → LUMO 74%, HOMO-2 → LUMO 15%
501.08	0.0043	HOMO-1 → LUMO 97%
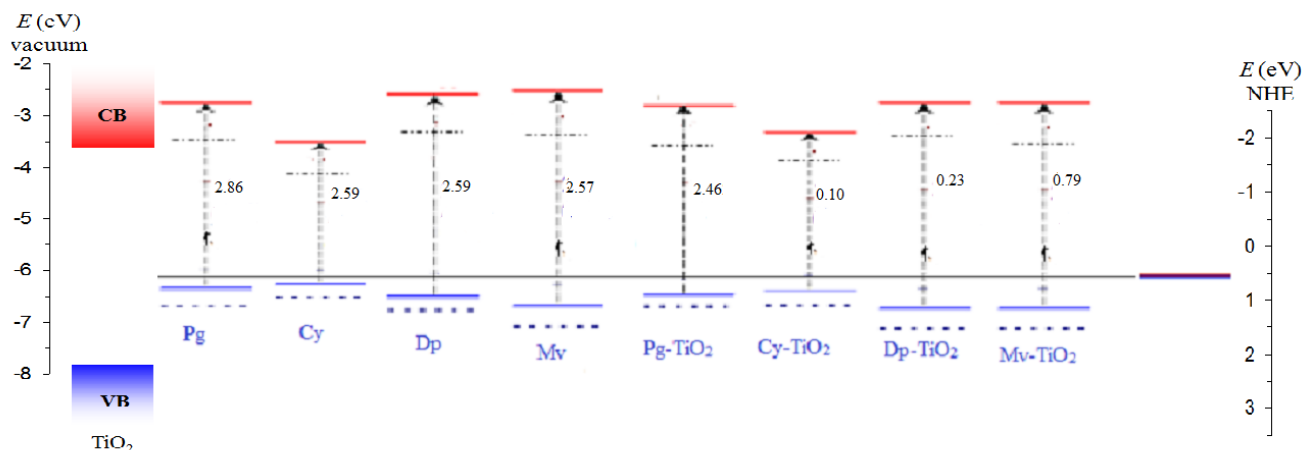
Figure 5: Energy diagram showing the ground state (blue lines) and the excited state (red lines) energies for the dyes, semiconductor and the dye-semiconductor couples. The conduction (red) and valence (blue) bands of the TiO_2, as well as the redox level of the I_3^-/I^- electrolyte are also shown on the left and right hand side, respectively.
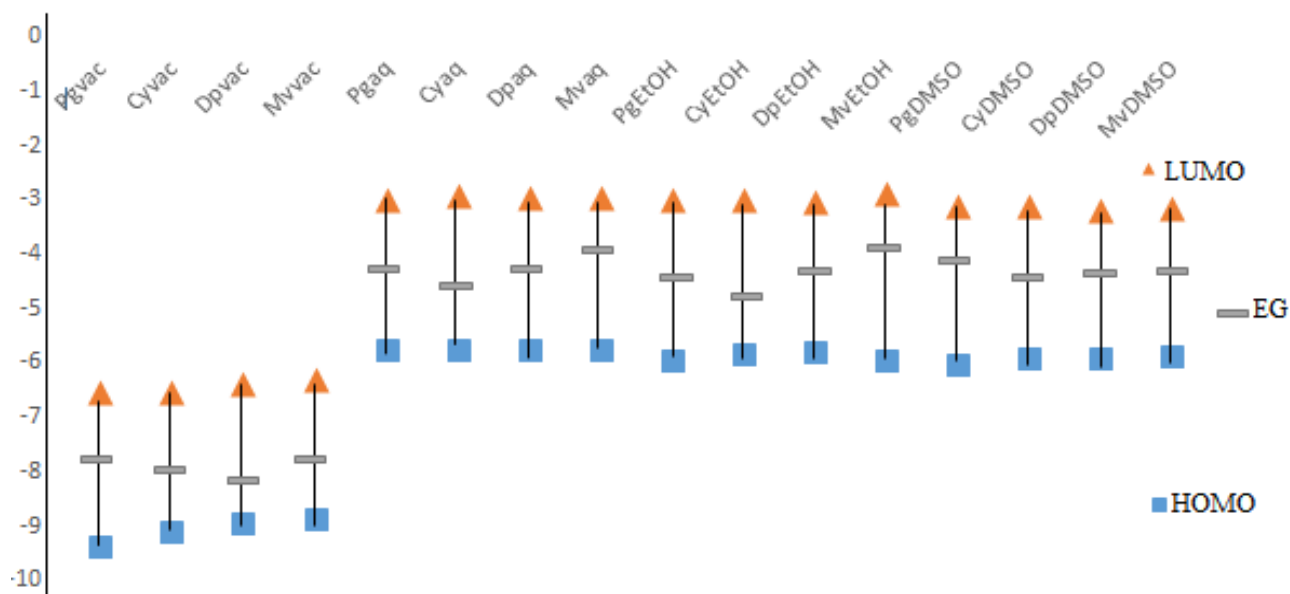

Figure 6: Energy diagram (HOMO, LUMO and energy bandgap) of dye-sensitizers in different media.

Notes: Cy, Dp, Mv and Pg are the abbreviations of the dye-sensitizers;, cyanidin, delphinidin malvidin and pelargonidin respectively. The vac., aq., EtOH and DMSO are respectively for the (gas, water, ethanol and dimethyl sulfoxide) media.

4.4   Reactivity descriptors and electronic properties of the dye molecules in different media for the dye, semiconductor and the dye-semiconductor couples

Table 2 contains, in addition to the electronic properties, the chemical potential (μ), chemical hardness (η) and light harvesting efficiency values obtained for the dye molecules in the gas phase. The chemical potential (μ), chemical hardness (η') semiconductor and dye-semiconductor couples in aqueous phase (aq), ethanol (EtOH) and dimethyl sulfoxide (DMSO). The effect of solvents on the calculated values of molecular global descriptors were correlated with the light harvesting efficiency of the dye molecules in the gas phase as shown in the graphical relationship between light harvesting efficiency and chemical hardness presented as Figure 7. Graphical relationship between light harvesting efficiency and chemical hardness is presented as Figure 7. It has been reported that the narrower gap between LHE and chemical hardness (η) correspond longer light absorption wavelength and effective CT of the dye-sensitizer (Semire *et al*., 2017). Chemical hardness, η which is related to the resistance to intramolecular charge transfer (Martsinovich & Troisi, 2011) is expected to be low in value for a dye to be desired in DSSCs. For the dye molecules employed as sensitizers in this study, the order of the distance of separation between the LHE and η is of the order Cy < Pg < Dp < Mv. This implies that the solar cell with Cy as sensitizer will be characterized with the longest light absorption wavelength and highest effective charge transfer among the four anthocyanidins. This is in agreement with the empirical data earlier obtained when pure anthocyanidins were applied as sensitizers in DSSCs (Abdulsalami *et al*., 2016).
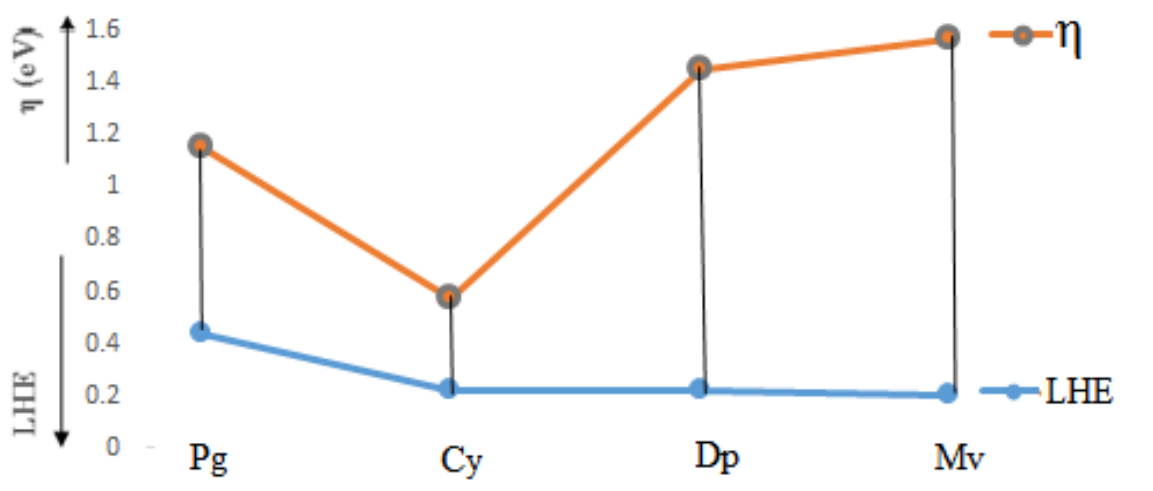
Figure 7: Relationship between light harvesting efficiency (LHE) and chemical hardness   for the studied dyes.

4.5   Local reactivity descriptors

Values obtained for condensed Fukui functions calculations oxygen atoms of the hydroxyl and methoxyl moieties are given by Fukui functions; $F_{(r)}^+$, $F_{(r)}^-$ and the dual descriptor; $\Delta F_{(r)}$ The values of these parameters are presented as Table 4. There are four to six oxygen atoms in the anthocyanidin molecules; Pg has four, Cy has five, Dp and Mv has six of such oxygen atoms each in their molecules, see Figure 6. The highest F^+ values obtained are 0.132 for O2 (Dp), 0.073 for O3 (Dp), 0.104 for O4 (Cy), 0.125 for O5 (Dp), 0.311for O6 (Dp) and 0.039 for O7 (Mv). The highest F^- values obtained are as follows; 0.136 (O2), 0.106 (O3), 0.107 (O4), 0.122 (O5), 0.113 (O6) and 0.071 (O7) for Cy, Pg, Cy, Cy, Cy and Dp respectively. The dual descriptors values obtained are as follows: Pg O2 has -0.0396, O3 has -0.314, O4 has -0.078 and O5 has -0.012; for Cy the values obtained are -0.131, -0.105, -0.002, -0.073 and -0.078 for O2, O3, O4, O5 and O6 respectively; Dp has 0.186, 0.141, 0.118, 0.178, 0.42 and 0.122 for the O2, O3, O4, O5, O6 and O7 respectively and 0.108, 0.128, -0.102, -0.075, -0.074 and -0.065 were obtained for O2, O3, O4, O5, O6 and O7 respectively for the oxygen (attached to the OH and OCH_3) moieties in Mv.

It is very imperative to consider the situation corresponding to a molecular centre that is going to receive a certain amount of charge at some other centre as well as a molecular center that is going to donate back a certain amount of charge through the same centre or another one (Gomez *et al.,* 2006). The values obtained for condensed Fukui functions calculations oxygen atoms of the hydroxyl and methoxyl moieties are given by f_k^+ and f_k^- and presented as Table 4. In the anthocyanidin molecules there are four to six oxygen atoms; Pg has four, Cy has five, Dp and Mv has six, Fukui function calculations were performed on each atoms in the molecules.

The highest value of F_k^- for O2 is found at Cy, O3 is found at Pg, O4, O5 and O6 are found on Cy, the highest value for O7 is found on Mv. For f_k^+ the highest values for O2, O3, O5, O6 and O7 are found on Dp, O4 is found on Cy. Dp represents most probable centres for nucleophillic attack in the molecules. The dual descriptor revealed that the O2 and O6 moieties of Cy molecules has the highest propensity to electrophilic attack, followed by Dp, then Mv and Dp. The propensity of nucleophilic attack is in the reverse. The energy diagram of the sensitizers in different media is presented as Figure 6. The energy bandgap values of Cy, Dp, Mv and Pg, in gas phase were found to be the lowest when compared to those found in other media. The energy bandgap in gas phase for the anthocyanidins were of the order Dp < Cy < Pg < Mv. In the aqueous, ethanol and dimethylsulphoxide (media) the values of bandgap were of the order Cy < Pg < Dp < Mv.

The calculated data obtained in media other than the gas phase were in agreement with the empirical and other theoretical data. The empirical data were obtained via solvent mixture and the theoretical calculations were carried out in media other than gas phase, in gas phase hyperfine transitions were being considered in the calculated data which were not catered for in the experimental.

	Atom	P_{N+1}	P_N	P_{N-1}	F^+	F^-	ΔF
Pg	O2	-0.641	-0.635	-0.668	-0.0066	0.033	-0.0396
	O3	-0.77	-0.562	-0.668	-0.208	0.106	-0.314
	O4	-0.705	-0.642	-0.657	-0.063	0.015	-0.078
	O5	-0.643	-0.641	-0.671	-0.002	0.03	-0.032
	O2	-0.564	-0.569	-0.705	0.005	0.136	-0.131
	O3	-0.573	-0.571	-0.674	-0.002	0.103	-0.105
	O4	0.548	-0.565	-0.67	0.107	0.105	0.002
	O5	-0.514	-0.563	-0.685	0.049	0.122	-0.073
	O6	-0.539	-0.574	-0.687	0.035	0.113	-0.078
	O2	-0.524	-0.656	-0.602	0.132	-0.054	0.186
	O3	-0.581	-0.654	-0.586	0.073	-0.068	0.141
	O4	-0.549	-0.642	-0.577	0.093	-0.065	0.158
	O5	-0.515	-0.64	-0.587	0.125	-0.053	0.178
	O6	-0.346	-0.657	-0.548	0.311	-0.109	0.42
	O7	-0.605	-0.676	-0.625	0.071	-0.051	0.122

Mv							
	O2	-0.520	-0.635	-0.642	0.115	0.007	0.108
	O3	-0.58	-0.650	-0.592	0.070	-0.058	0.128
	O4	-0.549	-0.506	-0.565	-0.043	0.059	-0.102
	O5	-0.516	-0.501	-0.561	-0.015	0.060	-0.075
	O6	-0.347	-0.322	-0.371	-0.025	0.049	-0.074
	O7	-0.399	-0.373	-0.412	-0.026	0.039	-0.065

In conclusion, theoretical data have been used to further enunciate the fact that thorough understanding of the chemistry of chromophores to be used as sensitizers in DSSs is important to address the issue of efficiency. Cy-sensitized solar cell has the highest efficiency among anthocyanidins and this is in agreement with reported empirical report.